



Published in final edited form as:

ACS Chem Biol. 2020 August 21; 15(8): 2041–2047. doi:10.1021/acscchembio.0c00114.

## Inhibition and Crystal Structure of the Human DHTKD1-Thiamin Diphosphate Complex

João Leandro<sup>†,‡</sup>, Susmita Khamrui<sup>§</sup>, Hui Wang<sup>§,||</sup>, Chalada Suebsuwong<sup>§,||</sup>, Natalia S. Nemeria<sup>⊥</sup>, Khoi Huynh<sup>§,||</sup>, Moses Moustakim<sup>§,||</sup>, Cody Secor<sup>§</sup>, May Wang<sup>†,‡</sup>, Tetyana Dodatko<sup>†,‡</sup>, Brandon Stauffer<sup>#</sup>, Christopher G. Wilson<sup>∇</sup>, Chunli Yu<sup>†,‡</sup>, Michelle R. Arkin<sup>∇</sup>, Frank Jordan<sup>⊥</sup>, Roberto Sanchez<sup>§,||</sup>, Robert J. DeVita<sup>§,||</sup>, Michael B. Lazarus<sup>§,\*</sup>, Sander M. Houten<sup>†,‡,\*</sup>

<sup>†</sup> Department of Genetics and Genomic Sciences, Icahn School of Medicine at Mount Sinai, New York, NY 10029, USA

<sup>‡</sup> Icahn Institute for Data Science and Genomic Technology, Icahn School of Medicine at Mount Sinai, New York, NY 10029, USA

<sup>§</sup> Department of Pharmacological Sciences, Icahn School of Medicine at Mount Sinai, New York, NY 10029, USA

<sup>||</sup> Drug Discovery Institute, Icahn School of Medicine at Mount Sinai, New York, NY 10029, USA

<sup>⊥</sup> Department of Chemistry, Rutgers, The State University of New Jersey, Newark, New Jersey 07102, USA

<sup>#</sup> Mount Sinai Genomics, Inc, Stamford, CT 06902, USA

<sup>∇</sup> Small Molecule Discovery Center and Department of Pharmaceutical Chemistry, University of California, San Francisco, CA 94143, USA

### Abstract

DHTKD1 is the E1 component of the 2-oxoadipate dehydrogenase complex, an enzyme involved in the catabolism of (hydroxy-)lysine and tryptophan. Mutations in *DHTKD1* have been associated with 2-aminoadipic and 2-oxoadipic aciduria, Charcot-Marie-Tooth disease type 2Q and eosinophilic esophagitis, but the pathophysiology of these clinically distinct disorders remains elusive. Here we report the identification of adipoylphosphonic acid and tenatoprazole as DHTKD1 inhibitors using targeted and high throughput screening, respectively. We furthermore elucidate the DHTKD1 crystal structure with thiamin diphosphate bound at 2.25 Å. We also report the impact of ten disease-associated missense mutations on DHTKD1. Whereas the majority of the

\*Corresponding Authors: michael.lazarus@mssm.edu, sander.houten@mssm.edu.

Author Contributions

Conceptualization, RJD, MBL, SMH; Methodology, BS, CGW, CY, MRA, FJ, RS, MBL, SMH; Investigation, JL, SK, HW, CSu, NSM, KH, MM, CS, MW, TD, CGW, MBL, SMH; Writing –Original Draft, JL, MBL, SMH; Writing –Review & Editing, JL, MRA, MBL, SMH; Funding Acquisition, MRA, RJD, MBL, SMH.

The authors declare no competing financial interest.

Supporting Information

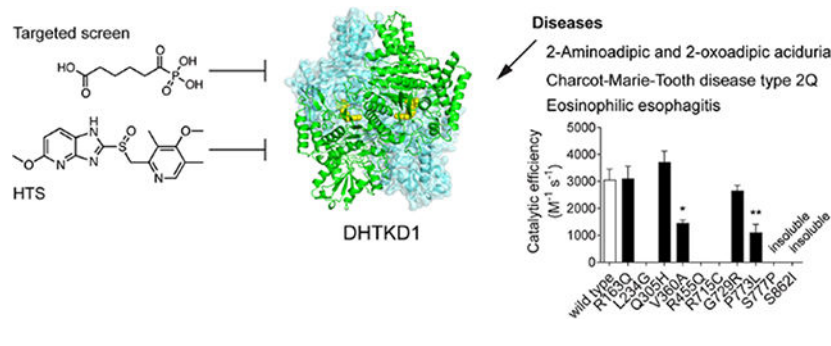
The Supporting Information is available free of charge via the Internet at <http://pubs.acs.org>.

Supplementary methods, supplementary Figures S1–S13 and Tables S1–S3.

PyMOL session (ZIP): DHTKD1 docking complex of OA and docking complex of adipoylphosphonic acid.

DHTKD1 variants displayed impaired folding or reduced thermal stability in combination with absent or reduced enzyme activity, three variants showed no abnormalities. Our work provides chemical and structural tools for further understanding of the function of DHTKD1 and its role in several human pathologies.

## Graphical Abstract



## INTRODUCTION

DHTKD1 is the E1 component (E1a) of the 2-oxoadipate dehydrogenase complex (OADHc) that operates in L-lysine, L-hydroxylysine and L-tryptophan degradation and converts 2-oxoadipic acid (OA) into glutaryl-CoA (Figure S1).<sup>1–7</sup> DHTKD1 is a homolog of 2-oxoglutarate dehydrogenase (OGDH, ~39% identity), the E1 component (E1o) of the 2-oxoglutarate dehydrogenase complex (OGDHc) that functions in the citric acid cycle. In general, 2-oxo acid dehydrogenase complexes have unique E1 and E2 components, but share the same E3 component. DHTKD1 and OGDH are an exception, because they share both the E2 (DLST) and E3 (DLD) components.<sup>4, 5, 8</sup>

Genetic studies have implicated DHTKD1 in the pathogenesis of three distinct human diseases. Autosomal recessive mutants in *DHTKD1* cause 2-aminoadipic and 2-oxoadipic aciduria (AMOXAD; MIM 204750),<sup>2, 3, 6</sup> a biochemical abnormality of questionable clinical significance that is characterized by the accumulation of 2-aminoadipic acid (AA) and OA (Figure S1).<sup>9</sup> Autosomal dominant variants have been associated with Charcot-Marie-Tooth disease type 2Q (CMT2Q, MIM 615025) and eosinophilic esophagitis (EoE).<sup>10–12</sup> There is currently no satisfactory pathophysiological mechanism that explains the observed pleiotropy of *DHTKD1* variants. A structure to model the consequences of the observed amino acid substitutions is currently not available. Homologous structures have been resolved for *Escherichia coli* E1o (sucA) and *Mycobacterium smegmatis* KGD (2-oxoglutarate decarboxylase),<sup>13–15</sup> which respectively share 40% and 37% identity with DHTKD1. Both proteins adopt the common fold of thiamin diphosphate (ThDP)-dependent 2-oxo acid dehydrogenases.<sup>16, 17</sup>

The function of OADHc is upstream of glutaryl-CoA dehydrogenase, the enzyme defective in glutaric aciduria type 1 (GA1; MIM 231670).<sup>18</sup> The limited clinical consequences of AMOXAD led to the hypothesis that inhibition of DHTKD1 is a potential therapeutic strategy to treat GA1.<sup>2, 8, 19</sup> Unfortunately, the substantial substrate overlap between

OGDHc and OADHc precludes a significant reduction in the accumulation of toxic substrates.<sup>8, 19</sup> Nevertheless, inhibitors are useful tools that will help to understand the function of this enzyme and its role in human disease. Here we report the crystal structure of the first human DHTKD1 at 2.25 Å in complex with ThDP and identify the first drug-like inhibitors of the enzyme.

## RESULTS AND DISCUSSION

In order to be able to screen for DHTKD1 inhibitors, we optimized an assay based on dichlorophenolindophenol (DCPIP) reduction (Figure S2A). We first assessed substrate specificity of DHTKD1 by measuring the activity with 2-oxoglutaric acid (OG), OA, 2-oxopimelic acid (OP) and 2-oxosuberic acid (OS), which vary only in carbon chain length (Figures 1A and 1B). Consistent with the genetic evidence and work by others,<sup>2, 4, 7</sup> we found that DHTKD1 has optimal activity with OA (Figure S1) and negligible activity with OG and OS. Interestingly, DHTKD1 also displayed activity with OP, a metabolite currently unknown in human metabolism. Although the affinity of DHTKD1 for OP was lower than for OA, the  $V_{max}$  appeared higher with OP (Figure 1A and Figure S2B). In addition, the activity with OA declined much more rapidly than the activity with OP providing a better dynamic window in inhibitor screening assays (Figure S2C).

Six out of the 23 selected substrate analogs were able to inhibit DHTKD1 (Table S1). OG and OS inhibited DHTKD1 activity competitively (Figure 1B, Figure S2D and Table S1). These data indicate that while DHTKD1 prefers OA and OP as substrates, OG and OS are able to bind to the enzyme, which is consistent with previous work.<sup>4</sup> Vigabatrin, an anti-epileptic known to cause  $\alpha$ -aminoaciduria,<sup>20</sup> did not inhibit DHTKD1, but its oxo analog 4-oxo-5-hexenoic acid inhibited DHTKD1 irreversibly (Figure 1B). OG, OS and 4-oxo-5-hexenoic acid had relatively low affinities for DHTKD1.

Interestingly, *in vitro* reconstituted OADHc (DHTKD1, DLST and DLD) shows activity toward OG.<sup>4</sup> This apparent inconsistency is likely explained by differences in the assayed enzyme reactions. OADHc relies on the E2 component DLST for oxidation and transfer of the enamine intermediate to lipoic acid and ultimately CoA. This reaction will not only be determined by the substrate specificity of DHTKD1, but also by that of DLST. Given the canonical role of DLST in the OGDHc, it should work well with succinyl intermediates (3-carboxy-1-hydroxypropyl-ThDP) possibly facilitating DHTKD1 to convert OG. Binding of OG to DHTKD1 is supported by the observation that it acts as a competitive inhibitor in the DHTKD1 specific enzyme assay.

Succinylphosphonic acid is a known inhibitor of OGDHc.<sup>4, 21</sup> Phosphonic acids inhibit 2-oxo acid dehydrogenase complexes by forming a pre-decarboxylation nucleophilic adduct at the C2 thiazolium atom that resembles a transition state analog.<sup>22–24</sup> We evaluated the ability of succinyl-, glutaryl-, adipoyl- and pimeloyl-phosphonic acid to inhibit DHTKD1. Adipoylphosphonic acid (AP) was a highly effective and specific mixed competitive-noncompetitive inhibitor of DHTKD1 ( $K_i$  of  $0.15 \pm 0.03 \mu\text{M}$ ), whereas glutaryl- and pimeloylphosphonic acid were less effective and succinyl-phosphonic acid was ineffective (Figures 1B and 1C and Figures S2E–G). We next assessed the ability of AP to inhibit

human OGDHc and OADHc containing OGDH and DHTKD1, respectively (Figures S2H–K). AP inhibited OADHc activity with an estimated  $K_i^{\text{app}}$  of  $0.105 \pm 0.038 \mu\text{M}$ . Taking into account that the inhibitor and substrate bind in the same active centers, the  $K_i$  was an estimated 1.6 nM indicating a tight-binding inhibitor (Figure 1B and Figure S2J). These data indicate that AP is a potent inhibitor of OADHc and not of OGDHc (Figures S2J and S2K), which establishes that it is the E1 component that is subject to inhibition by AP rather than the E2 or E3 components.

We next used circular dichroism (CD) to monitor the formation of 1',4'-iminophosphoadipoyl-ThDP at  $\sim 305\text{nm}$ , a reporter of the tetrahedral predecarboxylation intermediate in ThDP-dependent enzymes.<sup>23–25</sup> We showed that the positive  $\text{CD}_{305}$  signal depended on the concentration of AP (Figures S2L–N) and displayed saturation of the DHTKD1 active centers by AP at a molar ratio of 1.87 (with much less or no saturation of the OGDH active centers (Figures S2O–S)). These data demonstrate stoichiometric binding of AP in the active centers of DHTKD1, a finding that correlates with the loss of OADHc activity. Thus, AP is a mechanism-based, active-center-directed potent, tight-binding inhibitor of DHTKD1. To test whether this compound could inhibit DHTKD1 in cells, we treated HEK-293 cells and looked at the levels of AA, the transamination product of the DHTKD1 substrate OA (Figure S1). AP dose-dependently increased the level of AA in HEK-293 cells, demonstrating the successful inhibition of DHTKD1 (Figures S3A and S3B). Smaller changes were observed in other amino acids mainly at higher concentrations of AP (Figure S3B).

In order to identify DHTKD1 inhibitors with drug-like properties, we developed and performed a high-throughput screen (HTS, Figures S4–S7). The class of compounds that were consistently identified as DHTKD1 inhibitors in the screen were benzimidazole and imidazopyridine proton-pump inhibitors, with tenatoprazole being most potent ( $\text{IC}_{50}$ ,  $27 \pm 1 \mu\text{M}$ ) (Figure 1D). Analysis of sulfone and sulfide analogs of omeprazole and pantoprazole respectively, highlighted the importance of the sulfoxide group in the DHTKD1 inhibition process (Figure S8). Tenatoprazole displayed kinetics most compatible with a noncompetitive inhibition of DHTKD1 ( $K_i = 83 \pm 34 \mu\text{M}$ ) (Figure 1D and Figures S9A and S9B). We then analyzed the drug-protein interaction by differential scanning fluorimetry (DSF). Surprisingly, tenatoprazole destabilized the protein, decreasing the melting temperature by over 3 degrees ( $250 \mu\text{M}$ ) or 5 degrees ( $500 \mu\text{M}$ ) (Figure 1E and Figure S9C), an effect absent in the presence of dithiothreitol (DTT, Figure S9D). AP stabilized the protein in the same assay (Figure S9E). We compared the other omeprazole analogs in the same assay and found that destabilization tracked with the  $\text{IC}_{50}$  values of the inhibitors, with tenatoprazole showing the largest destabilization of all the compounds (Figure 1E). We note that the unusually large destabilization of DHTKD1 by tenatoprazole indicates structural alterations upon binding. We were unable to co-crystallize tenatoprazole with DHTKD1 in the same crystal form consistent with the possibility that tenatoprazole alters the conformation of the protein. Tenatoprazole was unable to inhibit OADHc, likely due to the presence of DTT in the assay mixture. Tenatoprazole dose-dependently increased AA levels in cells (Figure 1F) with smaller changes in some other amino acids (Asn, Met, Leu and His), indicating the inhibition of DHTKD1 is rather specific (Figure S9F).

No eukaryotic structures have been reported for E1o homologs. We obtained a crystal structure of human DHTKD1 at 2.25 Å (PDB code 6U3J) (Figures 2A and S10) using the *M. smegmatis* KGD structure as a search model for molecular replacement. The cofactor ThDP was present and bound to several highly conserved residues in the active site, making key presumed hydrogen bonds (Figure 2B). These contacts include N366 and D333 from the GDG/A motif, which coordinate the magnesium ion, and L290, which helps enforce the unusual conformation of ThDP, and E640, which is involved in the tautomerization of the 4'-aminopyrimidine ring in ThDP.<sup>26, 27</sup>

DHTKD1 crystallized as a dimer (Figure 2A and Table S2), similar to the *M. smegmatis* homolog, with the two monomers twisted around each other and two active sites formed at the interface. We believe that the minimal functional unit is a dimer, which is evidenced by several observations. First, we note that each of the two active sites in the dimer comprises residues from both copies of the protein, with one chain providing residues for binding the phosphate moieties and the other for the thiamin (Figure 2B). It is unlikely that a single copy can bind ThDP fully. Secondly, we found a previously unreported magnesium coordinating E641 from each monomer, which is suggestive of a stable ionic interaction (Figure 2C). The *M. smegmatis* homolog has two phenylalanines at this position while the *E. coli* one also has glutamates, although no magnesium was reported in the *E. coli* structure. Thirdly, we note that the surface area of the interface between the two monomers is extensive. According to the PISA server, the interface covers over 5000 Å<sup>2</sup> of area with a predicted  $\Delta G$  of -29.6 kcal/mol, suggestive of a strong interaction between the two copies.<sup>28</sup> It is likely that the full complex stabilizes the dimer further.

The tightly packed dimer still leaves room for the substrates to be solvent accessible, so they can be transferred to the other components of the complex (Figure S11A). While the active site is conserved between *M. smegmatis* and human (Figure S11B), we note two major differences. The human protein has a smaller serine (S288) in the active site instead of tyrosine, which provides more room compared to the *M. smegmatis* protein (Figures S11C and S11D), which may explain the ability of the protein to accept larger substrates such as OA and OP. Additionally human DHTKD1 has a Tyr residue at position 190, which differs from the Phe residue found in the *M. smegmatis* protein and other proteins of the OGDH family, and is predicted to be implicated in substrate binding. We studied the possible binding mode of OA, OP and adipoylphosphonic acid by docking the compounds into the DHTKD1 structure. Using induced fit docking (IFD), to allow for small adjustments in the protein structure, we obtained binding modes for OA and OP that are compatible with the formation of a pre-decarboxylation intermediate at the C2 thiazolium atom of ThDP (Figure S11E, SI PyMOL session and not shown). The substrate is positioned in the active site by a series of hydrogen bonding interactions with the side chains of K188, Y190, H435, N436, and H708. IFD of the adipoylphosphonic acid inhibitor showed that it mimics the substrate binding mode resulting in a pose that is compatible with the formation of the decarboxylation nucleophilic adduct suggested by the experimental data (Figure S11F and SI PyMOL session). We expressed the Y190F and S288Y mutant proteins, as well as the Y190F/S288Y double mutant to evaluate the effect on substrate affinity (Figures S12A and S12B). We obtained very little soluble full-length protein for the double mutant, which was inactive with OP. The Y190F and S288Y mutant proteins expressed well. The  $V_{\max}$  of the

Y190F mutant was decreased for both the OA and OP substrates, but the decrease was more distinct for the larger OP (Figure S12C). The  $K_m$  was only increased for OA, but ultimately the decrease of the catalytic efficiency ( $k_{cat}/K_m$ ) was most pronounced for OP. Both wild type (WT) and Y190F protein displayed very little activity with OG. The S288Y mutant protein was inactive with all substrates (Figure S12C). Thus the tested single amino acid replacements do not fully account for the observed differences in substrate specificity of human DHTKD1 and *M. smegmatis* KGD. Other (neutral) amino acid substitutions are likely needed for compensatory interactions, although the data are consistent with the importance of Y190 for substrate binding.

Next, we studied all reported missense variants in DHTKD1 (Figure 3A) (7 variants reported in AMOXAD patients<sup>2, 3, 6</sup> and 3 variants associated with EoE)<sup>11</sup> (Figures S13A and S13B). The S777P and S862I variants were largely insoluble and the small amounts of soluble protein exhibited severe proteolysis during expression and purification. This indicates that the mutations prevent proper folding of the protein. In the crystal structure, the S862 sidechain makes important contacts to sidechains in two different parts of the protein, T917 and H812. Losing these contacts and inserting the bulkier hydrophobic isoleucine likely inhibits protein folding. For S777, there is a hydrogen bond between the serine sidechain and the backbone of neighboring L589. The mutation at this position eliminates this interaction as well as introduces a proline, which can destabilize the current backbone conformation due to its different preference in  $\phi, \psi$  dihedral angles.

Three variants displayed a higher propensity to form insoluble protein (L234G, R455Q and R715C), but enough soluble protein was recovered to establish that they were inactive. For the remaining 5 DHTKD1 variants, we determined steady-state kinetic parameters (Table 1, Figures S13C and S13D). Substrate affinity was not changed in any of the variants. Two variants (V360A and P773L) showed a consistent decrease in  $V_{max}$ , whereas no changes were observed for the other variants (R163Q, Q305H and G729R). The decreased  $V_{max}$  for V360A and P773L may be related to a lower percentage of active protein after purification caused by decreased  $T_m$  values (see below). In addition, less full-length protein was purified for P773L.

The observed DHTKD1 variants are spread throughout the protein and generally avoid the ThDP binding site (Figure 3A). All 8 soluble variants were stable enough to determine the melting temperature by DSF testing (Figure 3B). Q305H and G729R had statistically insignificant changes on the  $T_m$  of the protein suggesting that their effects are not structural. L234G, V360A, and P773L had decreased  $T_m$  values. V360 is in the core of the protein and reducing its size likely destabilizes the hydrophobic packing of the protein as observed in other enzymes.<sup>29</sup> L234G and P773L likely cause problems in folding by altering to glycine or from proline, which have unique dihedral angle preferences. The remaining 3 variants had relatively small, but reproducible changes with an increase in stability for R455Q and R715C, and a decrease in stability for R163Q. R455 forms a salt bridge with D400 and a hydrogen bond with T430 while R715 makes a salt bridge with D677 and a hydrogen bond with Q673. Mutation of these residues likely abrogates activity by disrupting these important interactions.

The majority of variants displayed impaired folding or reduced thermal stability in combination with absent or reduced enzyme activity providing a likely mechanism for loss-of-function as observed in AMOXAD. Fibroblasts from an AMOXAD patient with compound heterozygosity for R455Q/S777P did not display any immunoreactivity for DHTKD1,<sup>3</sup> which is consistent with our analysis of these two variants. For Q305H and G729R, however, protein folding and activity appear unaffected, but the genetic evidence for their causality is strong. Indeed recent work revealed that OADHc containing DHTKD1 with p.G729R is inactive due to changes in the assembly with the E2 component and resulting defective substrate channeling.<sup>30</sup> Q305 is near the surface but makes important internal contacts, so it is unclear how it could maintain activity, but perhaps the substitution to His maintains these contacts but interferes with formation of OADHc. Future studies should focus on the function of OADHc containing this variant.

The three autosomal dominant missense variants associated with EoE have quite distinct properties. R163Q behaves similar to the WT protein, V360A had a lower  $V_{max}$  and thermal stability and S862I was insoluble. EoE is a chronic allergic inflammatory esophageal disorder and it remains unclear how DHTKD1 variants can produce a dominant effect leading to mitochondrial dysfunction as implicated in the pathogenesis of this disease.<sup>11</sup> A possible effect on the assembly of the OADHc and the recently described hybrid complex with OGDHc<sup>8</sup> remains to be demonstrated. Alternatively, the EoE mutations could lead to a conformation-driven gain-of-function mechanism, as has recently been demonstrated for mutations in the aminoacyl-transfer RNA (tRNA) synthetases associated with CMT.<sup>31</sup>

In summary, we have determined the crystal structure of human DHTKD1, an enzyme associated with 3 clinically distinct disorders AMOXAD, CMT2Q and EoE. We have identified AP and tenatoprazole as specific inhibitors of this protein. Adipoylphosphonic acid lacks chemical properties to be developed as a drug, but we show it is a useful tool *in vitro* and in whole cell systems. Tenatoprazole is a proton pump inhibitor belonging to a class of acid-activated prodrugs that inhibit the gastric H,K-ATPase.<sup>32</sup> Given this and its rather low potency as DHTKD1 inhibitor, tenatoprazole is likely not useful in future studies on DHTKD1 function without further optimization. Lastly, we have determined the consequences of all DHTKD1 missense variants reported to date, which combined with the human structure, allowed us to begin to understand the role of DHTKD1 in human disease.

## METHODS

A complete description of methods is included in the Supporting Information.

## Supplementary Material

Refer to Web version on PubMed Central for supplementary material.

## ACKNOWLEDGMENT

Research reported in this publication was supported by the Eunice Kennedy Shriver National Institute of Child Health & Human Development of the National Institutes of Health (NIH) under Award Number R03HD092878 (to S.M.H.) and R21HD088775 (to S.M.H. and R.J.D.) and R35GM124838 (to M.B.L.) and by grant UL1TR001433 from the National Center for Advancing Translational Sciences, NIH. This research used resources of the National

Synchrotron Light Source II, a U.S. Department of Energy (DOE) Office of Science User Facility operated for the DOE Office of Science by Brookhaven National Laboratory under Contract No. DE-SC0012704. The Life Science Biomedical Technology Research resource is primarily supported by the NIH, National Institute of General Medical Sciences (NIGMS) through a Biomedical Technology Research Resource P41 grant (P41GM111244), and by the DOE Office of Biological and Environmental Research (KP1605010).

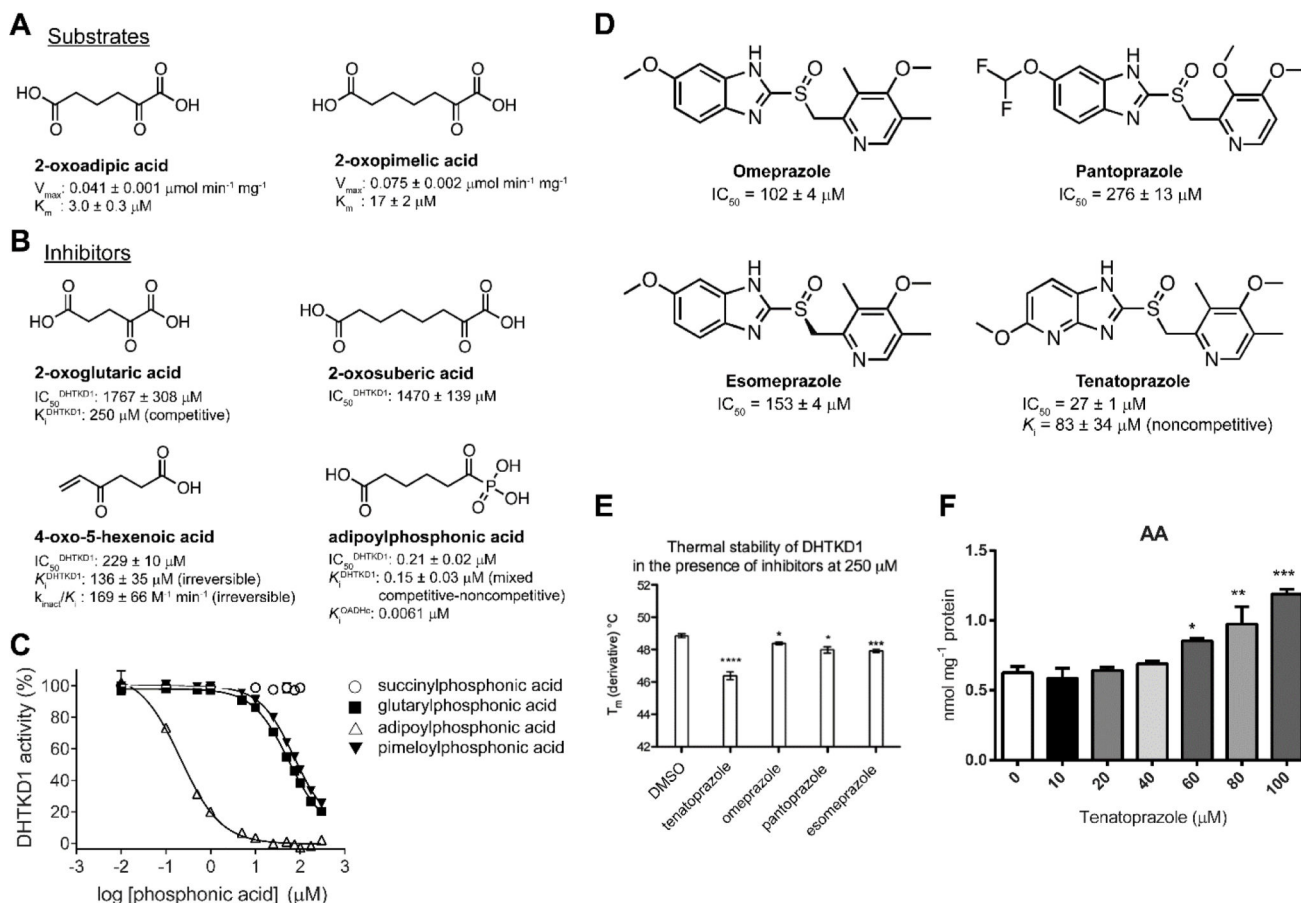
## REFERENCES

- (1). Bunik VI, and Degtyarev D (2008) Structure-function relationships in the 2-oxo acid dehydrogenase family: substrate-specific signatures and functional predictions for the 2-oxoglutarate dehydrogenase-like proteins. *Proteins* 71, 874–890. [PubMed: 18004749]
- (2). Danhauser K, Sauer SW, Haack TB, Wieland T, Stauffner C, Graf E, Zschocke J, Strom TM, Traub T, Okun JG, Meitinger T, Hoffmann GF, Prokisch H, and Kolker S (2012) DHTKD1 mutations cause 2-aminoadipic and 2-oxoadipic aciduria. *Am. J. Hum. Genet.* 91, 1082–1087. [PubMed: 23141293]
- (3). Hagen J, te Brinke H, Wanders RJ, Knecht AC, Oussoren E, Hoogeboom AJ, Ruijter GJ, Becker D, Schwab KO, Franke I, Duran M, Waterham HR, Sass JO, and Houten SM (2015) Genetic basis of alpha-aminoadipic and alpha-ketoadipic aciduria. *J. Inherit. Metab. Dis.* 38, 873–879. [PubMed: 25860818]
- (4). Nemeria NS, Gerfen G, Nareddy PR, Yang L, Zhang X, Szostak M, and Jordan F (2018) The mitochondrial 2-oxoadipate and 2-oxoglutarate dehydrogenase complexes share their E2 and E3 components for their function and both generate reactive oxygen species. *Free Radic. Biol. Med.* 115, 136–145. [PubMed: 29191460]
- (5). Nemeria NS, Gerfen G, Yang L, Zhang X, and Jordan F (2018) Evidence for functional and regulatory cross-talk between the tricarboxylic acid cycle 2-oxoglutarate dehydrogenase complex and 2-oxoadipate dehydrogenase on the l-lysine, l-hydroxylysine and l-tryptophan degradation pathways from studies in vitro. *Biochim. Biophys. Acta Bioenerg.* 1859, 932–939. [PubMed: 29752936]
- (6). Stiles AR, Venturoni L, Mucci G, Elbalalesy N, Woontner M, Goodman S, and Abdenur JE (2016) New Cases of DHTKD1 Mutations in Patients with 2-Ketoadipic Aciduria. *JIMD Rep.* 25, 15–19. [PubMed: 26141459]
- (7). Wu Y, Williams EG, Dubuis S, Mottis A, Jovaisaite V, Houten SM, Argmann CA, Faridi P, Wolski W, Kutalik Z, Zamboni N, Auwerx J, and Aebersold R (2014) Multilayered genetic and omics dissection of mitochondrial activity in a mouse reference population. *Cell* 158, 1415–1430. [PubMed: 25215496]
- (8). Leandro J, Dodatko T, Aten J, Nemeria NS, Zhang X, Jordan F, Hendrickson RC, Sanchez R, Yu C, DeVita RJ, and Houten SM (2020) DHTKD1 and OGDH display substrate overlap in cultured cells and form a hybrid 2-oxo acid dehydrogenase complex in vivo. *Hum. Mol. Genet.* 29, 1168–1179. [PubMed: 32160276]
- (9). Goodman SI, and Duran M (2014) Biochemical phenotypes of questionable clinical significance In *Physician's guide to the diagnosis, treatment, and follow-up of inherited metabolic diseases* (Blau N, Duran M, Gibson KM, and Dionisi-Vici C, Eds.), pp 691–705, Springer Verlag: Heidelberg.
- (10). Dohrn MF, Glockle N, Mulahasanovic L, Heller C, Mohr J, Bauer C, Riesch E, Becker A, Battke F, Hortnagel K, Hornemann T, Suriyanarayanan S, Blankenburg M, Schulz JB, Claeys KG, Gess B, Katona I, Ferbert A, Vittore D, Grimm A, Wolking S, Schols L, Lerche H, Korenke GC, Fischer D, Schrank B, Kotzaeridou U, Kurlemann G, Drager B, Schirmacher A, Young P, Schlotter-Weigel B, and Biskup S (2017) Frequent genes in rare diseases: panel-based next generation sequencing to disclose causal mutations in hereditary neuropathies. *J. Neurochem.* 143, 507–522. [PubMed: 28902413]
- (11). Sherrill JD, Kc K, Wang X, Wen T, Chamberlin A, Stucke EM, Collins MH, Abonia JP, Peng Y, Wu Q, Putnam PE, Dexheimer PJ, Aronow BJ, Kottyan LC, Kaufman KM, Harley JB, Huang T, and Rothenberg ME (2018) Whole-exome sequencing uncovers oxidoreductases DHTKD1 and OGDHL as linkers between mitochondrial dysfunction and eosinophilic esophagitis. *JCI Insight* 3.



- (12). Xu WY, Gu MM, Sun LH, Guo WT, Zhu HB, Ma JF, Yuan WT, Kuang Y, Ji BJ, Wu XL, Chen Y, Zhang HX, Sun FT, Huang W, Huang L, Chen SD, and Wang ZG (2012) A nonsense mutation in DHTKD1 causes Charcot-Marie-Tooth disease type 2 in a large Chinese pedigree. *Am. J. Hum. Genet.* 91, 1088–1094. [PubMed: 23141294]
- (13). Frank RA, Price AJ, Northrop FD, Perham RN, and Luisi BF (2007) Crystal structure of the E1 component of the Escherichia coli 2-oxoglutarate dehydrogenase multienzyme complex. *J. Mol. Biol.* 368, 639–651. [PubMed: 17367808]
- (14). Wagner T, Barilone N, Alzari PM, and Bellinzoni M (2014) A dual conformation of the post-decarboxylation intermediate is associated with distinct enzyme states in mycobacterial KGD (alpha-ketoglutarate decarboxylase). *Biochem. J.* 457, 425–434. [PubMed: 24171907]
- (15). Wagner T, Bellinzoni M, Wehenkel A, O'Hare HM, and Alzari PM (2011) Functional plasticity and allosteric regulation of alpha-ketoglutarate decarboxylase in central mycobacterial metabolism. *Chem. Biol.* 18, 1011–1020. [PubMed: 21867916]
- (16). Åvarsson A, Chuang JL, Wynn RM, Turley S, Chuang DT, and Hol WG (2000) Crystal structure of human branched-chain alpha-ketoacid dehydrogenase and the molecular basis of multienzyme complex deficiency in maple syrup urine disease. *Structure* 8, 277–291. [PubMed: 10745006]
- (17). Arjunan P, Nemeria N, Brunskill A, Chandrasekhar K, Sax M, Yan Y, Jordan F, Guest JR, and Furey W (2002) Structure of the pyruvate dehydrogenase multienzyme complex E1 component from Escherichia coli at 1.85 Å resolution. *Biochemistry* 41, 5213–5221. [PubMed: 11955070]
- (18). Larson A, and Goodman S (2019) Glutaric Acidemia Type 1. In *GeneReviews*((R)) (Adam MP, Ardinger HH, Pagon RA, Wallace SE, Bean LJH, Stephens K, and Amemiya A, Eds.), Seattle (WA).
- (19). Biagosch C, Ediga RD, Hensler SV, Faerberboeck M, Kuehn R, Wurst W, Meitinger T, Kolker S, Sauer S, and Prokisch H (2017) Elevated glutaric acid levels in Dhtkd1-/Gcdh- double knockout mice challenge our current understanding of lysine metabolism. *Biochim. Biophys. Acta Mol. Basis Dis* 1863, 2220–2228. [PubMed: 28545977]
- (20). Vallat C, Rivier F, Bellet H, Magnan de Bornier B, Mion H, and Echenne B (1996) Treatment with vigabatrin may mimic alpha-aminoadipic aciduria. *Epilepsia* 37, 803–805. [PubMed: 8764822]
- (21). Bunik VI, Denton TT, Xu H, Thompson CM, Cooper AJ, and Gibson GE (2005) Phosphonate analogues of alpha-ketoglutarate inhibit the activity of the alpha-ketoglutarate dehydrogenase complex isolated from brain and in cultured cells. *Biochemistry* 44, 10552–10561. [PubMed: 16060664]
- (22). Artiukhov AV, Graf AV, and Bunik VI (2016) Directed Regulation of Multienzyme Complexes of 2-Oxo Acid Dehydrogenases Using Phosphonate and Phosphinate Analogs of 2-Oxo Acids. *Biochemistry (Mosc.)* 81, 1498–1521. [PubMed: 28259128]
- (23). Nemeria N, Chakraborty S, Baykal A, Korotchkina LG, Patel MS, and Jordan F (2007) The 1',4'-iminopyrimidine tautomer of thiamin diphosphate is poised for catalysis in asymmetric active centers on enzymes. *Proc. Natl. Acad. Sci. U. S. A.* 104, 78–82. [PubMed: 17182735]
- (24). Nemeria NS, Chakraborty S, Balakrishnan A, and Jordan F (2009) Reaction mechanisms of thiamin diphosphate enzymes: defining states of ionization and tautomerization of the cofactor at individual steps. *FEBS J.* 276, 2432–2446. [PubMed: 19476485]
- (25). Baykal AT, Kakalis L, and Jordan F (2006) Electronic and nuclear magnetic resonance spectroscopic features of the 1',4'-iminopyrimidine tautomeric form of thiamin diphosphate, a novel intermediate on enzymes requiring this coenzyme. *Biochemistry* 45, 7522–7528. [PubMed: 16768448]
- (26). Hawkins CF, Borges A, and Perham RN (1989) A common structural motif in thiamin pyrophosphate-binding enzymes. *FEBS Lett.* 255, 77–82. [PubMed: 2792374]
- (27). Jordan F, Nemeria NS, Zhang S, Yan Y, Arjunan P, and Furey W (2003) Dual catalytic apparatus of the thiamin diphosphate coenzyme: acid-base via the 1',4'-iminopyrimidine tautomer along with its electrophilic role. *J. Am. Chem. Soc.* 125, 12732–12738. [PubMed: 14558820]
- (28). Krissinel E, and Henrick K (2007) Inference of macromolecular assemblies from crystalline state. *J. Mol. Biol.* 372, 774–797. [PubMed: 17681537]

- (29). Xu J, Baase WA, Baldwin E, and Matthews BW (1998) The response of T4 lysozyme to large-to-small substitutions within the core and its relation to the hydrophobic effect. *Protein Sci.* 7, 158–177. [PubMed: 9514271]
- (30). Zhang X, Nemeria NS, Leandro J, Houten S, Lazarus MB, Gerfen GJ, Ozohanics O, Ambrus A, Nagy B, Brukh R, and Jordan F (2020) Structure-function analyses of the G729R 2-oxoadipate dehydrogenase genetic variant associated with a disorder of L-lysine metabolism. *J. Biol. Chem.* 295, 8078–8095. [PubMed: 32303640]
- (31). Blocquel D, Sun L, Matuszek Z, Li S, Weber T, Kuhle B, Kooi G, Wei N, Baets J, Pan T, Schimmel P, and Yang XL (2019) CMT disease severity correlates with mutation-induced open conformation of histidyl-tRNA synthetase, not aminoacylation loss, in patient cells. *Proc. Natl. Acad. Sci. U. S. A.* 116, 19440–19448. [PubMed: 31501329]
- (32). Shin JM, and Sachs G (2008) Pharmacology of proton pump inhibitors. *Curr. Gastroenterol. Rep.* 10, 528–534. [PubMed: 19006606]

**Figure 1.**

Substrates and inhibitors of DHTKD1. (A) Structure of DHTKD1 substrates and their kinetic parameters. (B) Structure and  $IC_{50}$ ,  $K_i$  and  $k_{inact}/K_i$  (for irreversible inhibitors) of DHTKD1 inhibitors. (C) DHTKD1 inhibition by phosphonic acids. (D) Proton-pump inhibitors are inhibitors of DHTKD1. Structures,  $IC_{50}$  and  $K_i$  of selected proton-pump inhibitors. (E) Thermal stability of DHTKD1 with  $250 \mu\text{M}$  proton-pump inhibitors. (F) Tenatoprazole inhibits DHTKD1 in HEK-293 cells. \* $P < 0.05$ , \*\* $P < 0.01$  and \*\*\* $P < 0.001$ .

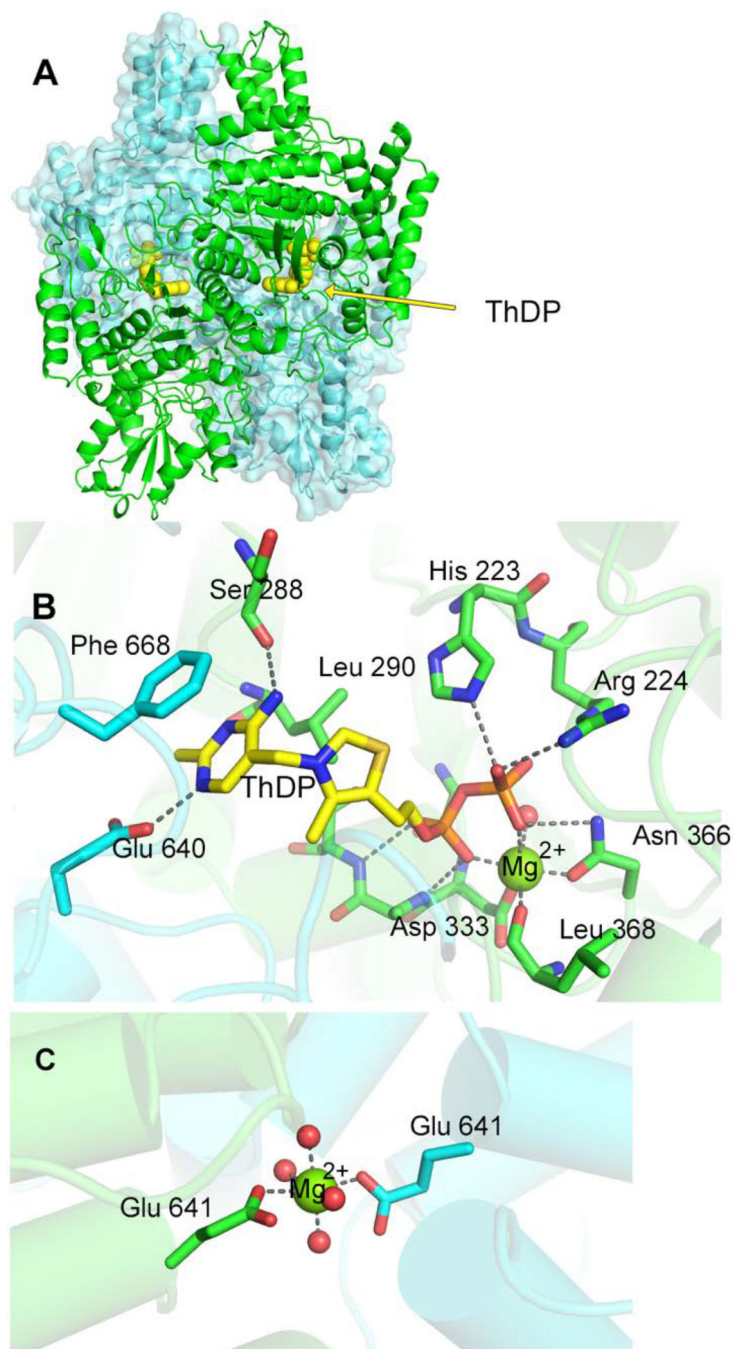


**Figure 2.** Crystal structure of human DHTKD1 complexed to ThDP. (A) Overall fold of DHTKD1. The dimer is shown with one chain in green and the other in cyan, with the ThDP cofactor shown in yellow. (B) Active site of human DHTKD1. Several interactions that help bind ThDP and the magnesium ion are indicated. Residues are colored according to the chain they come from. (C) Dimeric magnesium interface. Coordination of one glutamate from each monomer by a magnesium ion is shown, with the rest of the octahedral magnesium

sites coordinated to water. The magnesium was assigned based on the octahedral geometry observed.

Author Manuscript

Author Manuscript

Author Manuscript

Author Manuscript

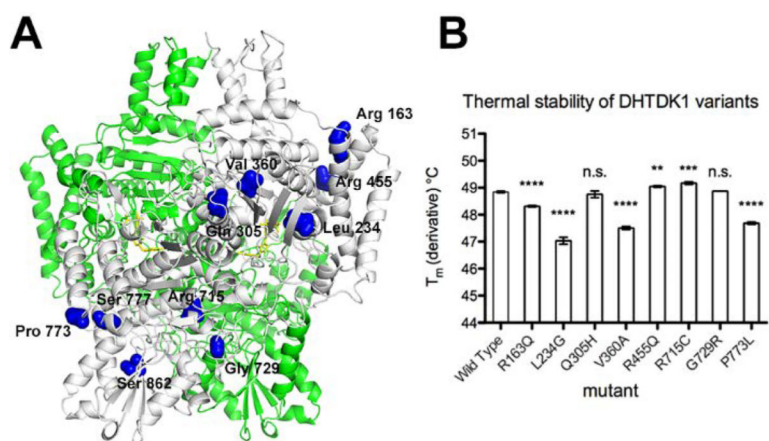


**Figure 3.** DHTKD1 variants. (A) Structural localization of DHTKD1 missense variants analyzed. Amino acid residues affected by mutations are indicated as spheres in dark blue on one monomer. (B) Thermal stability of DHTKD1 variants.

**Table 1.**

Steady-state kinetic properties of wild type and variant DHTKD1 proteins.

DHTKD1		$V_{\max}$	$k_{\text{cat}}$	$K_{\text{m}}$	$k_{\text{cat}}/K_{\text{m}}^a$
		( $\mu\text{mol DCPIPH}_2 \cdot \text{min}^{-1} \cdot \text{mg}^{-1}$ )	( $\text{s}^{-1}$ )	( $\mu\text{M}$ )	( $\text{M}^{-1} \cdot \text{s}^{-1}$ )
–	WT	0.041 ± 0.004	0.138 ± 0.012	47 ± 3	3056 ± 400
c.488G>A	p.R163Q (EoE) <sup>b</sup>	0.044 ± 0.004	0.146 ± 0.014	49 ± 7	3106 ± 449
c.700_701delinsGG	p.L234G	inactive			
c.915G>C	p.Q305H	0.045 ± 0.005	0.151 ± 0.015	41 ± 5	3715 ± 413
c.1079T>C	p.V360A (EoE)	0.024 ± 0.002 ( $p = 0.02$ )	0.082 ± 0.006 ( $p = 0.02$ )	57 ± 5	1450 ± 112 ( $p = 0.02$ )
c.1364G>A	p.R455Q	inactive			
c.2143C>T	p.R715C	inactive			
c.2185G>A	p.G729R	0.034 ± 0.005	0.115 ± 0.016	43 ± 4	2656 ± 201
c.2318C>T	p.P773L	0.014 ± 0.002 ( $p = 0.0005$ )	0.049 ± 0.006 ( $p = 0.0005$ )	47 ± 6	1105 ± 297 ( $p = 0.006$ )
c.2329 T>C	p.S777P	n.a. <sup>c</sup>			
c.2585G>T	p.S862I (EoE)	n.a.			

Values represent mean ± SEM and  $p$  values are indicated when a variant value differed significantly from the WT.

<sup>a</sup>The catalytic efficiency ( $k_{\text{cat}}/K_{\text{m}}$ ) was calculated on the basis of dimer molecular mass of 201 kDa for the DHTKD1 processed form after removal of the mitochondrial transit peptide.

<sup>b</sup>Mutations detected in patients with EoE; all others were observed in AMOXAD patients.

<sup>c</sup>n.a., not available due to the lack of solubility of the protein.